

Zinc transporter 3 modulates cell proliferation and neuronal differentiation in the adult hippocampus

Bo Young Choi¹ | Dae Ki Hong¹ | Jeong Hyun Jeong¹ | Bo Eun Lee¹ |
Jae-Young Koh² | Sang Won Suh¹ 

¹Department of Physiology, Hallym University
College of Medicine, Chuncheon, South Korea

²Department of Neurology, University of
Ulsan College of Medicine, Seoul, South Korea

Correspondence

Sang Won Suh, MD, PhD, Department of
Physiology, Hallym University, College of
Medicine, 1 Hallymdaehak-gil, Chuncheon,
24252, South Korea.
Email: swsuh@hallym.ac.kr

Funding information

National Research Foundation of Korea,
Grant/Award Numbers:
NRF-2017M3C7A1028937,
NRF-2019R1A2C4004912,
NRF-2020R1A2C2008480

Abstract

The subgranular zone of the dentate gyrus is a subregion of the hippocampus that has two uniquely defining features; it is one of the most active sites of adult neurogenesis as well as the location where the highest concentrations of synaptic zinc are found, the mossy fiber terminals. Therefore, we sought to investigate the idea that vesicular zinc plays a role as a modulator of hippocampal adult neurogenesis. Here, we used *ZnT3*^{-/-} mice, which are depleted of synaptic-vesicle zinc, to test the effect of targeted deletion of this transporter on adult neurogenesis. We found that this manipulation reduced progenitor cell turnover as well as led to a marked defect in the maturation of newborn cells that survive in the DG toward a neuronal phenotype. We also investigated the effects of zinc (ZnCl₂), n-acetyl cysteine (NAC), and ZnCl₂ plus 2NAC (ZN) supplement on adult hippocampal neurogenesis. Compared with ZnCl₂ or NAC, administration of ZN resulted in an increase in proliferation of progenitor cells and neuroblast. ZN also rescued the *ZnT3* loss-associated reduction of neurogenesis via elevation of insulin-like growth factor-1 and ERK/CREB activation. Together, these findings reveal that *ZnT3* plays a highly important role in maintaining adult hippocampal neurogenesis and supplementation by ZN has a beneficial effect on hippocampal neurogenesis, as well as providing a therapeutic target for enhanced neuroprotection and repair after injury as demonstrated by its ability to prevent aging-dependent cognitive decline in *ZnT3*^{-/-} mice. Therefore, the present study suggests that *ZnT3* and vesicular zinc are essential for adult hippocampal neurogenesis.

KEYWORDS

adult neurogenesis, hippocampus, n-acetyl cysteine, zinc, zinc transporter 3

1 | INTRODUCTION

The divalent cationic zinc (Zn²⁺) is the second most abundant transition metal in the brain and spinal cord following iron and is a major player in

numerous cellular and physiological processes.¹ Most ionic zinc in the brain is tightly bound with proteins such as metallothionein or metalloproteins.² Loosely bound or free-zinc is often found at increased concentrations in synaptic vesicles in brain regions where neurogenesis and

This is an open access article under the terms of the Creative Commons Attribution-NonCommercial License, which permits use, distribution and reproduction in any medium, provided the original work is properly cited and is not used for commercial purposes.

©2020 The Authors. STEM CELLS published by Wiley Periodicals, Inc. on behalf of AlphaMed Press 2020

neural migration actively occur in the adult brain, such as the hippocampal dentate gyrus (DG) and olfactory bulb.^{3,4} Zinc is a component of over 300 enzymes and highly involved in the regulation of cell division and DNA synthesis.⁵ Zinc deficiency leads to impaired DNA synthesis and growth retardation in animals.⁶ Zinc also influences hormonal regulation of cell division, such as that mediated by insulin-like growth factor-1 (IGF-1) or nerve growth factor.⁷ Several studies have reported the adverse effects of an insufficient supply of zinc on normal physiological function. Dietary zinc deprivation impairs performance in visual-attention and short-term-memory tasks.⁸ Taken together, the evidence suggests that zinc is an essential element for maintaining normal neuronal cell proliferation, development, and cognitive function.

The role of zinc transporter 3 (*ZnT3*) and vesicular zinc on cognitive function have been investigated by several labs. Adlard et al reported that *ZnT3*^{-/-} mice exhibit age-dependent deficits in learning and memory.⁹ Sindreu et al demonstrated that *ZnT3*^{-/-} mice have impaired contextual discrimination and spatial working memory.¹⁰ Martel et al showed that *ZnT3*^{-/-} mice performed normally at initial learning but showed difficulty finding a second platform location. These *ZnT3*^{-/-} mice display enhanced social interaction but were likewise strikingly poor at forming social and object recognition memory. Therefore, it appears that *ZnT3* is involved in spatial memory and behavior that relies on the hippocampus and perirhinal cortex.¹¹

Although the above studies reported that *ZnT3*^{-/-} mice showed learning and memory deficits during the aging process the precise mechanism is not clear. Thus, we hypothesized that deletion of *ZnT3* gene negatively affects adult hippocampal neurogenesis. To determine whether synaptic zinc is an important factor for modulating hippocampal neurogenesis, the present study also used *ZnT3*^{-/-} mice. We demonstrate a severe reduction of progenitor cell proliferation and neuronal differentiation in the DG of *ZnT3*^{-/-} mice. We propose a cell-extrinsic mechanism of *ZnT3* deficiency mediated by decreasing levels of IGF-1 and phosphorylation of both extracellular signal-regulated kinase (ERK) and cyclic AMP response element binding protein (CREB) in the hippocampus of *ZnT3*^{-/-} mice. The present study suggests that *ZnT3*^{-/-} mice display reduced hippocampal neurogenesis under physiological conditions even at 3 months of age. Our findings indicate that vesicular zinc plays an important role in adult hippocampal neurogenesis and have implications for cognitive health in aging and disease.

2 | MATERIALS AND METHODS

2.1 | Animals and ethics statement

ZnT3^{+/+} and *ZnT3*^{-/-} male mice (a kind gift from Dr Jae-Young Koh, Department of Neurology, University of Ulsan College of Medicine, Korea; background strains, C57BL/6 and Sv129 hybrid), aged 3 months (25-30 g) or 15-18 months (30-45 g), were bred and maintained in the facility of University of Hallym College of Medicine. The animals were housed in a temperature- and humidity-controlled environment (22°C ± 2°C, 55% ± 5% and a 12 hours light:12 hours dark cycle), supplied with Purina diet (Purina, Gyeonggi, Korea) and water ad libitum. Animal use

Significance statement

This study tested the hypothesis that *ZnT3* and vesicular zinc serve a critical role in the regulation of adult hippocampal neurogenesis. It was demonstrated that *ZnT3*^{-/-} mice display reduced hippocampal neurogenesis under physiological conditions, even at 3 months of age. The findings reveal that *ZnT3* has a central function in maintaining adult hippocampal neurogenesis and zinc supplementation by ZN has a beneficial effect on hippocampal neurogenesis and may offer a means to enhance neuroprotection and repair after injury.

and relevant experimental procedures were approved by the Institutional Animal Care and Use Committee, Hallym University (Protocol # Hallym 2017-16). This manuscript was written up in accordance with the ARRIVE (Animal Research: Reporting in vivo Experiments) guidelines.¹² Before all experiments, genotyping for *ZnT3* was performed using PCR with a primer set to amplify WT (5'-GGT ATC CAT GCC CTT CCT CTA GAG-3'), or common (5'-ATA GTC ACT GGC ATC CTC CTG TAC C-3'), or the KO allele (5'-CCT GTG CTC TAG TAG CTT TAC GG-3') as described previously.¹³

2.2 | Experimental design and 5-bromo-2-deoxyuridine labeling

To test the role of vesicular zinc at different stages of adult neurogenesis, we conducted 4-phase studies using *ZnT3*^{-/-} mice and zinc supplementation. In phase 1, to assess the effects of eliminating vesicular zinc at the early or late phase of adult hippocampal neurogenesis, mice were divided into two groups in each phase: *ZnT3*^{+/+} (n = 7) and *ZnT3*^{-/-} (n = 9). The thymidine analog BrdU (50 mg/kg; Sigma Cat# B5002, St. Louis, Missouri) was intraperitoneally injected twice daily for four consecutive days and the brains were harvested at 5 days (early phase) or 6 weeks (late phase) after the initial BrdU injection. In phase 2, to evaluate the effects of zinc supplementation at the early or late phase of adult hippocampal neurogenesis, mice were divided into four groups in each phase: vehicle (Veh; early phase, n = 10; late phase, n = 6), zinc chloride (ZnCl₂; early phase, n = 10; late phase, n = 8), n-acetyl cysteine (NAC; early phase, n = 11; late phase, n = 9), and ZnCl₂ plus 2NAC (ZN; early phase, n = 10; late phase, n = 9). Mice were given ZnCl₂ (4 mg/kg), NAC (20 mg/kg), or ZN intraperitoneally available once per day for 2 (early phase) or 8 weeks (late phase). BrdU was injected two times per day for four consecutive days starting 10 days after the initial ZN treatment, and then mice were sacrificed after the last dose of ZN. Control mice were injected with equal volumes of saline only (vehicle). In phase 3, zinc supplementation by ZN was initiated at the early or late phase of adult hippocampal neurogenesis and mice were divided into four groups in each phase: vehicle-treated *ZnT3*^{+/+} mice (early phase, n = 6; late

phase, $n = 6$), ZN-treated $ZnT3^{+/+}$ mice (early phase, $n = 9$; late phase, $n = 8$), vehicle-treated $ZnT3^{-/-}$ mice (early phase, $n = 6$; late phase, $n = 7$), ZN-treated $ZnT3^{-/-}$ mice (early phase, $n = 7$; late phase, $n = 6$). Mice were given ZN intraperitoneally once per day for 2 or 8 weeks. BrdU was injected two times per day for four consecutive days starting 10 days after initial ZN treatment, then mice were sacrificed at 2 (early phase) or 8 weeks (late phase) after initial ZN treatment. In phase 4, to analysis the effects of zinc supplementation by ZN on cognitive abilities, mice were divided into four groups: (a) vehicle-treated aged $ZnT3^{+/+}$ mice ($n = 11$), (b) vehicle-treated aged $ZnT3^{-/-}$ mice ($n = 13$), (c) ZN-treated aged $ZnT3^{+/+}$ mice ($n = 12$), and (d) ZN-treated aged $ZnT3^{-/-}$ mice ($n = 14$). ZN supplementation was performed once per day for 8 weeks. Morris water maze (MWM) test were conducted for six consecutive days starting 50 days after the initial ZN supplementation, then mice were sacrificed after the last dose of ZN.

2.3 | Quantitative analysis

To quantify BrdU-, Ki67-, DCX-, and pCREB-positive cells, every sixth coronal section spanning the septal hippocampus was collected. The number of BrdU-, Ki67-, DCX-, and pCREB-positive cells was determined in the subgranular zone (SGZ) and granular cell layer (GCL) from both hemispheres using optical fractionators probe unbiased stereology investigation (Stereo Investigator, MicroBrightField, Williston, Vermont).^{14,15} Counting frames ($15 \times 15 \times 20 \mu\text{m}$) were placed at the intersection of a matrix ($40 \times 40 \mu\text{m}$) randomly superimposed onto the region of interest by the program. Cells were counted using a $\times 63$ oil objective. To analyze the phenotype of the BrdU-positive cells, as mentioned previously, fluorescence signals were detected using a Zeiss LSM 710 confocal microscopy (Carl Zeiss, Oberkochen, Germany) with a sequential scanning mode for Alexa 488 and 594. Stacks of images (1024×1024 pixels) from consecutive slices of 0.9 to 1.2 μm in thickness were obtained by averaging eight scans per slice and were processed using ZEN 2 (Carl Zeiss). The number of BrdU⁺NeuN⁺ cells was estimated by multiplying the percentages of colocalization (determined by confocal microscopy) to the total number of BrdU-labeled cells (determined by stereology).

To measure IGF-1-immunofluorescence intensity, CA1, CA3, or DG from the brain section images were selected as regions of interest (ROIs) and measured using ImageJ. Briefly, the image was loaded into ImageJ, and changed into 8-bit via the menu option (Image/Color/Split Channels). The image was binarized, and the menu option (Analyze/Measure) was selected, and then immunofluorescence signal was expressed as the mean gray value.

To analyze the levels of pERK and TSQ intensity, DG and mossy fibers (MF) from the brain section images were selected as ROIs and measured using ImageJ. The image was converted to 8-bit through the menu options (Image/Type/8-bit). Next, an image threshold was set as follows (Image/Adjust/Threshold): the type was set to black and white and the bottom slider moved to a value sufficient to show only the pERK immunoreactive area or TSQ signal. The thresholded image was binary and only represented pERK immunoreactivity or TSQ signal. The selected part in the whole image was sorted, and

then, the intensity of pERK or TSQ was represented as the mean gray value.

2.4 | Statistical analysis

For statistical comparisons between $ZnT3^{+/+}$ and $ZnT3^{-/-}$ mice from phase 1, significance was evaluated using an unpaired Student's *t* test. The intensity data of immunostaining, Western blot, and TSQ staining from phase 2 to 3 were analyzed by Kruskal-Wallis test with post hoc analysis using Bonferroni correction to compare the values among four groups since the values did not meet normal distribution. The remaining immunohistochemical data, Western blot and probe trial data from phases 2 to 4 were analyzed by a one-way analysis of variance (ANOVA; $ZnT3^{-/-}$ or $ZnT3^{+/+}$ mice) \times (ZN or vehicle) with a post hoc Bonferroni multiple comparison test using statistical package for the social sciences (SPSS, Chicago, Illinois). Repeated measure ANOVA was used to examine the contribution of treatment and day on the escape latency. All data were expressed as the mean \pm SE and *P* value $< .05$ were considered significant. We then performed a post hoc power analysis with means, standard deviation, and number of subjects for four groups using G*Power 3.1.9.7.¹⁶ The result revealed that we obtained a power of 0.99. Therefore, our study design had sufficient power to reveal statistical significance in our study.

3 | RESULTS

3.1 | Vesicular zinc is eliminated in the hippocampus of $ZnT3^{-/-}$ mice

We determined mouse genotype by PCR. PCR analysis of genomic DNA shows loss of the *ZnT3* band (650 bp) and presence of the NEO cassette (400 bp) in the $ZnT3^{-/-}$ mice (Figure 1A). We also stained brain sections of $ZnT3^{+/+}$ and $ZnT3^{-/-}$ mice with the TSQ, zinc-specific fluorescent dye, to test whether vesicular zinc regulation is altered in $ZnT3^{-/-}$ mice. $ZnT3^{+/+}$ mice showed high intensity TSQ fluorescence signals in the hippocampal MF area. However, $ZnT3^{-/-}$ mice showed almost no fluorescence signals in the hippocampus (Figure 1B,B'). After examining TSQ fluorescence, we evaluated *ZnT3* immunoreactivity (IR) in both $ZnT3^{+/+}$ and $ZnT3^{-/-}$ mice. *ZnT3* localization on vesicle membranes was also lower in the hippocampus of $ZnT3^{-/-}$ mice. *ZnT3*-IR from $ZnT3^{-/-}$ mice was undetectable in the MFs of hippocampus (Figure 1C,C').

3.2 | Genetic deletion of *ZnT3* reduces hippocampal progenitor cell proliferation

To assess whether endogenous *ZnT3* affects DG progenitor cell proliferation, mice were injected with BrdU (50 mg/kg) twice per day for four consecutive days in both $ZnT3^{+/+}$ and $ZnT3^{-/-}$ mice (Figure 1D). We found that the BrdU- and Ki67-immunopositive cells were distributed mainly in the SGZ/GCL. A significant decrease in the number of

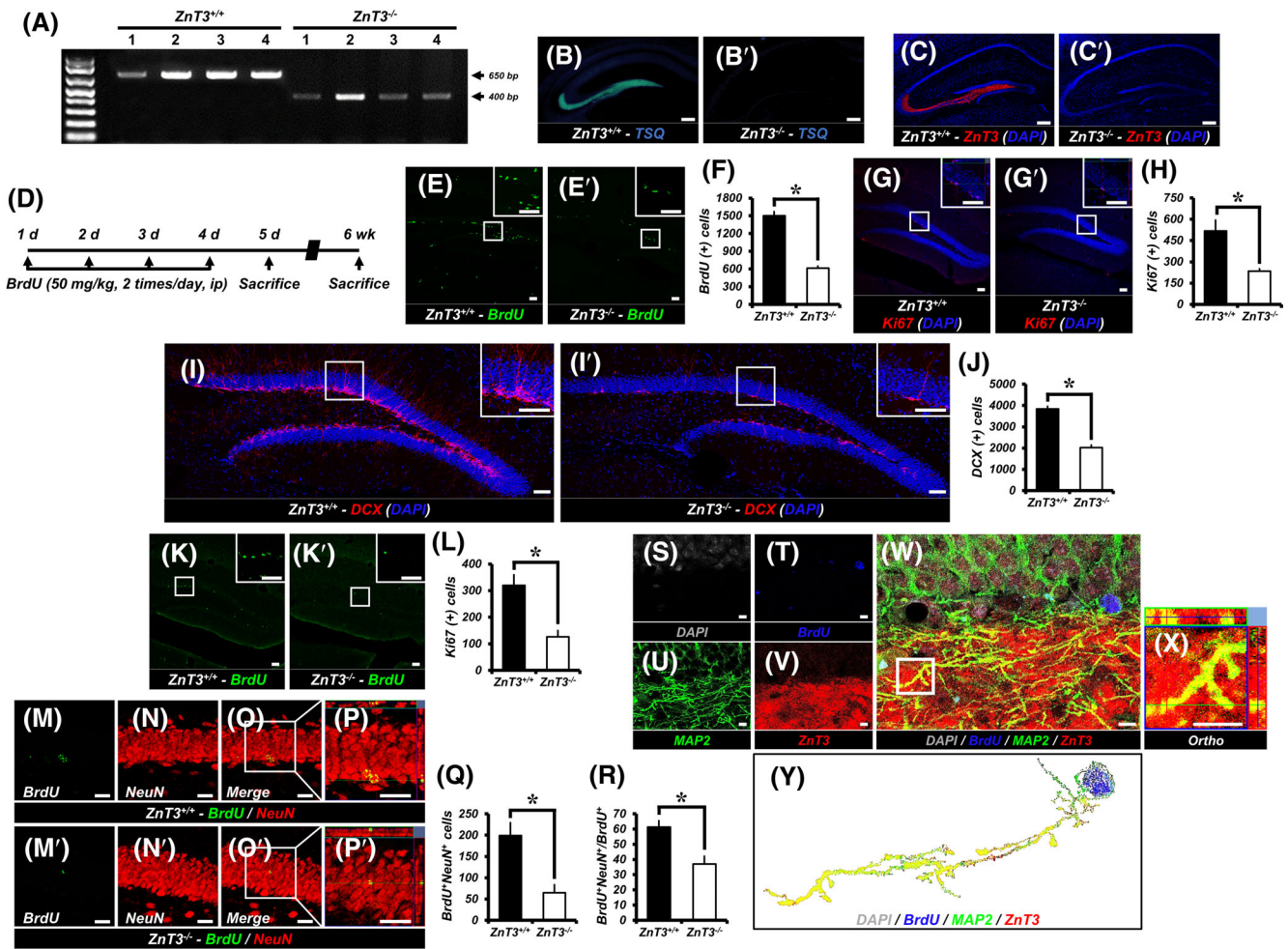


FIGURE 1 *Znt3*^{-/-} mice reduces adult hippocampal neurogenesis. A, Genotyping with PCR. PCR analysis of genomic DNA demonstrates the absence of the *Znt3* band (650 bp) and presence of the NEO cassette (400 bp) in *Znt3*^{-/-} mice. B-C', The distributions of TSQ-histofluorescence (B,B') and *Znt3*-immunoreactive fluorescence (C,C') were detected with TSQ and an anti-*Znt3* antibody. *Znt3*^{+/+} mice revealed high intensity of TSQ fluorescence and *Znt3*-immunoreactivity (IR) in the hippocampal mossy fiber area. However, *Znt3*^{-/-} mice did not show TSQ and *Znt3*-IR in the hippocampus. Scale bar = 200 μm. D, Timeline showing the experimental design. BrdU was intraperitoneally administered twice per day for four consecutive days. Mice were then killed at 5 days or 6 weeks after initial injection of BrdU. E,E', Representative images of the dentate gyrus (DG) showing BrdU (green) staining to *Znt3*^{+/+} (E) and *Znt3*^{-/-} (E') mice at 5 days after first injection of BrdU. Scale bar = 50 μm. F, Quantification of BrdU⁺ cells in the subgranular zone/granule cell layer (SGZ/GCL) (mean ± SEM; *Znt3*^{+/+}: n = 7; *Znt3*^{-/-}: n = 9). **P* < .05 (unpaired Student's *t* test). G,G', Representative images of Ki67- (red) and DAPI- (blue) immunopositive cells as merged images to *Znt3*^{+/+} (G) and *Znt3*^{-/-} (G') mice. Scale bar = 50 μm. H, Number of progenitor cells (Ki67⁺DAPI⁺) in the SGZ/GCL (mean ± SEM; *Znt3*^{+/+}: n = 7; *Znt3*^{-/-}: n = 9). **P* < .05 (unpaired Student's *t* test). I,I', Representative images of DCX- (red) and DAPI- (blue) immunopositive cells as merged images to *Znt3*^{+/+} (I) and *Znt3*^{-/-} (I') mice. Scale bar = 50 μm. J, Number of immature neurons (DCX⁺DAPI⁺) in the SGZ/GCL (mean ± SEM; *Znt3*^{+/+}: n = 7; *Znt3*^{-/-}: n = 9). **P* < .05 (unpaired Student's *t* test). K,K', Representative images of the DG showing BrdU (green) staining to *Znt3*^{+/+} (K) and *Znt3*^{-/-} (K') mice at 6 weeks after first injection of BrdU. Scale bar = 50 μm. L, Quantification of BrdU⁺ cells in the SGZ/GCL (mean ± SEM; *Znt3*^{+/+}: n = 7; *Znt3*^{-/-}: n = 9). **P* < .05 (unpaired Student's *t* test). M-P', Representative images of BrdU- (green) (M,M') and NeuN- (red) (N,N') immunopositive cells as merged images to *Znt3*^{+/+} (O,P) and *Znt3*^{-/-} (O',P') mice. Scale bar = 50 μm. Q,R, Bar graphs showing the number (Q) and percentage (R) of cells that express the markers BrdU and NeuN (newborn neurons) in the SGZ/GCL (mean ± SEM; *Znt3*^{+/+}: n = 7; *Znt3*^{-/-}: n = 9). **P* < .05 (unpaired Student's *t* test). S-Y, *Znt3* is expressed in newborn neurons. Representative immunofluorescence images showing DAPI- (gray) (S), BrdU- (blue) (T), MAP2- (green) (U), and *Znt3*- (red) (V) immunoreactive cells in the DG of *Znt3*^{+/+} mice at 6 weeks after initial BrdU injection as merged image (W). High-power view (X) showing colocalized *Znt3* immunoreactivity in axon of DAPI⁺BrdU⁺MAP2⁺ cells. Scale bar = 5 μm. Y, Representative image of the combined expression of *Znt3* and individual newborn neuron (DAPI⁺BrdU⁺MAP2⁺) using ImageJ

BrdU (Figure 1E,F) and Ki67 (Figure 1G,H) labeled cells was seen in the SGZ/GCL of *Znt3*^{-/-} mice as compared to age-matched *Znt3*^{+/+} mice at 5 days after first injection of BrdU. The *Znt3*^{-/-} mice had a 59.2% (BrdU) or 54.8% (Ki67) reduction of the hippocampal progenitor cell proliferation in comparison with controls.

3.3 | *Znt3*^{-/-} mice show reduced production of neuroblasts

To test whether *Znt3* influences the presence of immature neurons we performed immunostaining for DCX. Genetic deletion

of *ZnT3* caused a 47.3% reduction in the number of DCX-immunopositive cells, the specific marker of immature neurons (neuroblast) (Figure 1I,J).

3.4 | Compromised adult neurogenesis in the hippocampus of *ZnT3*^{-/-} mice

To investigate whether endogenous *ZnT3* influences survival of DG newborn cells, we birthdated newly generated cells in *ZnT3*^{+/+} and *ZnT3*^{-/-} mice by injecting BrdU twice daily for four consecutive days and investigated their fate at 6 weeks after initial BrdU injection. A significant decrease in the number of BrdU-labeled cells was seen in the SGZ/GCL of *ZnT3*^{-/-} mice (Figure 1K,L). The *ZnT3*^{-/-} mice had a 60.6% decrease in survival of newly generated cells in comparison with controls. We also calculated the ratio of the number of BrdU⁺ cells in the SGZ/GCL at 6 weeks to the number of BrdU⁺ cells in the DG at 5 days after initial BrdU injection and found that the survival ratio of BrdU-labeled cells in *ZnT3*^{-/-} mice (20.5%) was similar to that of controls (21.2%; data not shown).

Next, we determined the role of *ZnT3* on neuronal maturation of cells that survived in the SGZ/GCL at 6 weeks after initial BrdU injection. When calculating the number of adult newborn neurons, genetic deletion of *ZnT3* caused a significant decrease in the total number of BrdU⁺ cells double labeled for the specific marker of mature neurons (NeuN) in the SGZ/GCL (Figure 1M-Q). In addition, *ZnT3*^{-/-} mice showed a 39.52% decrease in the percentage of BrdU⁺NeuN⁺ cells in BrdU⁺ cells (Figure 1R). These results show that deletion of *ZnT3* decreases newborn mature neurons in the adult hippocampal DG.

3.5 | *ZnT3* is expressed in newly generated neurons

Next, we investigated whether *ZnT3* is expressed in newborn neurons in addition to mature neurons. To confirm the presence of *ZnT3* in newborn neurons, the DG of *ZnT3*^{+/+} mice at 6 weeks after initial BrdU injection were assayed via immunofluorescence staining for BrdU, *ZnT3*, and MAP2. We detected much stronger expression of *ZnT3* and MAP2 in the MF of DG. We also found that *ZnT3* protein colocalized with axons of BrdU⁺MAP2⁺ cells in the DG (Figure 1S-Y). This indicates that *ZnT3* is expressed in the axonal terminal of newborn neurons.

3.6 | ZN increases adult hippocampal neurogenesis

To determine whether ZN supplementation enhances adult hippocampal neurogenesis, we analyzed the effects of ZN supplementation on the rate of cell proliferation and neuronal differentiation within the DG (Figure 2A). Compared with vehicle-treated mice, the BrdU- and Ki67-labeled cells were not significantly changed in

ZnCl₂-treated mice, whereas NAC- or ZN-treated mice exhibited a significant increase in the number of BrdU- (Figure 2B-F) and Ki67-labeled cells (Figure 2G-K) in the SGZ. In addition, we also observed a greatly increased number of DCX-immunopositive cells in ZN-treated mice compared with vehicle, ZnCl₂ or NAC-treated mice (Figure 2L-P).

Furthermore, we also determined whether ZN supplementation increases levels of vesicular zinc in the hippocampal mossy fibers (MFs). We found that there were no differences in vesicular TSQ intensity between vehicle-treated and NAC-treated mice. However, vesicular TSQ intensity was increased in ZnCl₂-treated mice compared with vehicle-treated mice and ZN-treated mice showed significantly increased vesicular TSQ intensity in the MFs compared with vehicle-, ZnCl₂-, or NAC-treated mice (Figure 2Q,R).

We then explored whether ZN impacts the newly generated cell survival and neuronal maturation of newborn cells in the SGZ/GCL. ZN supplementation was performed once a day for 8 weeks. We injected BrdU twice per day for four consecutive days starting at 10 days after the initial ZN supplementation. The numbers of BrdU⁺ and BrdU⁺NeuN⁺ cells from mice treated with ZN were significantly higher than in sections from vehicle-, ZnCl₂-, or NAC-treated mice (Figure 2S-V). In addition, ZN-treated mice showed a significant increase in the percentage of BrdU⁺NeuN⁺ cells among BrdU⁺ cells (Figure 2W).

3.7 | ZN treatment reversed adult hippocampal neurogenesis in *ZnT3*^{-/-} mice

Here we sought to ascertain if the decline in progenitor cell proliferation and neuronal differentiation could be rescued by ZN. *ZnT3*^{+/+} and *ZnT3*^{-/-} mice were treated with ZN or vehicle (Figure 3A). We found that ZN treatment revealed an increase in the number of BrdU⁺, Ki67⁺ or DCX⁺ cells in the SGZ/GCL of both *ZnT3*^{+/+} and *ZnT3*^{-/-} mice compared with vehicle-treated mice, although *ZnT3*^{-/-} mice treated with ZN showed a lower number of BrdU⁺, Ki67⁺ or DCX⁺ cells than *ZnT3*^{+/+} mice treated with ZN (Figure 3B-G). These results show that ZN reverses the decrease in progenitor cell proliferation and neuroblast production, caused by genetic deletion of *ZnT3*.

We then explored whether ZN also impacts the survival of newly generated cells and the neuronal maturation of newborn cells that survive in the SGZ/GCL. ZN supplementation was performed once a day for 8 weeks. We injected BrdU twice per day for four consecutive days starting at 10 days after the initial ZN supplementation. The numbers of BrdU⁺ and BrdU⁺NeuN⁺ cells in *ZnT3*^{-/-} mice were significantly decreased in both vehicle- and ZN-treated groups, as compared to *ZnT3*^{+/+} mice. However, ZN treatment remarkably increased the numbers of BrdU⁺ and BrdU⁺NeuN⁺ cells in both *ZnT3*^{+/+} and *ZnT3*^{-/-} mice, as compared to vehicle-treated mice (Figure 3H-K). In addition, ZN treatment revealed an increase in the percentage of BrdU⁺NeuN⁺ cells among BrdU⁺ cells in both *ZnT3*^{+/+} and *ZnT3*^{-/-} mice compared with vehicle-treated mice, although

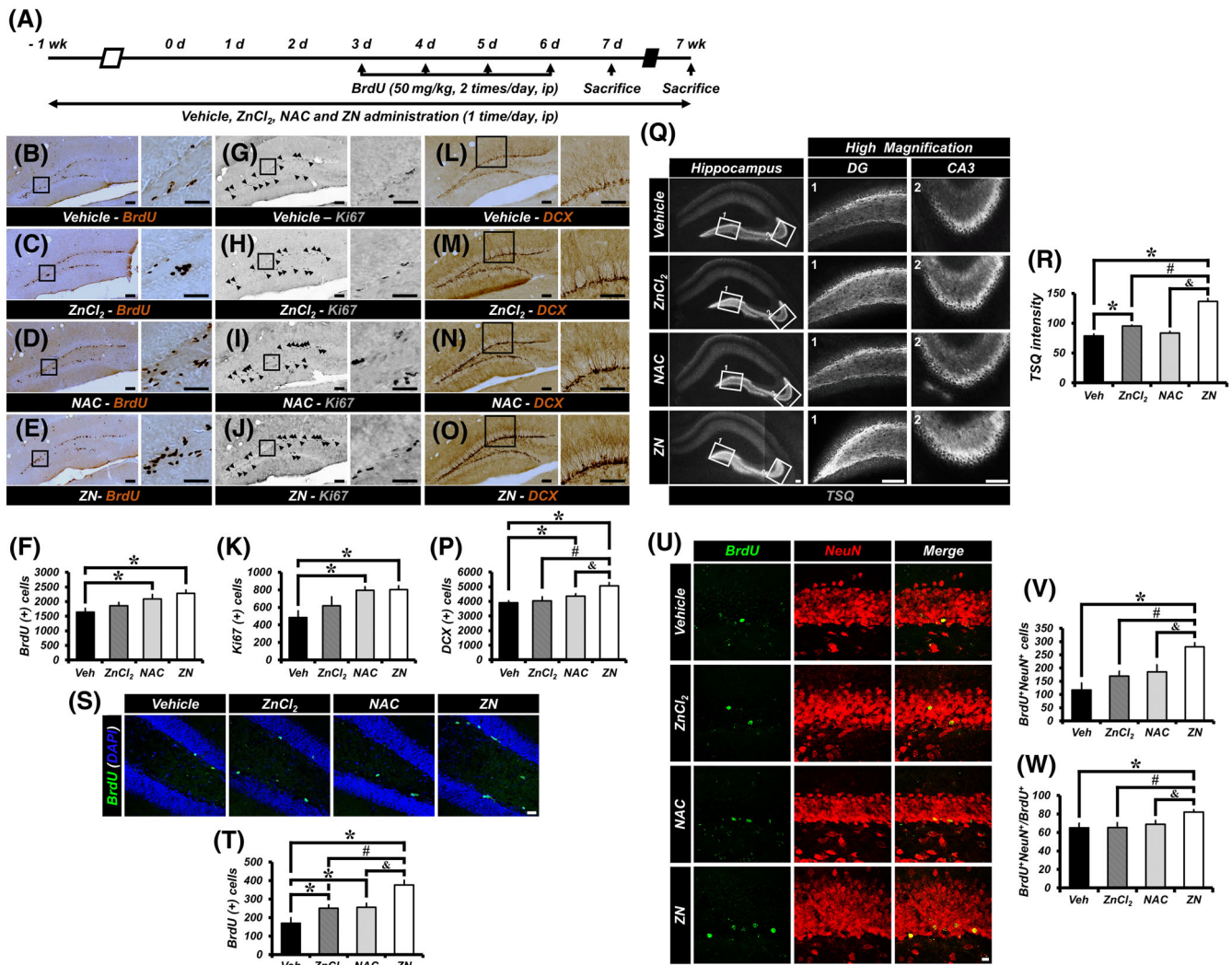


FIGURE 2 ZN increases adult hippocampal neurogenesis. A, Schematic of the experimental time course. B-E, Representative images of the DG showing BrdU staining to vehicle- (B), zinc chloride- ($ZnCl_2$) (C), n-acetyl cysteine- (NAC) (D) or $ZnCl_2$ + 2NAC- (ZN) (E) treated groups at 2 weeks after initial ZN supplementation. Scale bar = 50 μm . G-J, Representative images of Ki67-immunopositive cells to vehicle- (G), $ZnCl_2$ - (H), NAC- (I), or ZN- (J) treated groups. Scale bar = 50 μm . L-O, Representative images of DCX-immunopositive cells to vehicle- (L), $ZnCl_2$ - (M), NAC- (N), or ZN- (O) treated groups. Scale bar = 50 μm . F, K, P, Number of progenitor cells (BrdU⁺ [F] or Ki67⁺ [K]) and neuroblasts (DCX⁺ [P]) in the SGZ/GCL (mean \pm SEM; Veh, n = 10; $ZnCl_2$, n = 10; NAC, n = 11; ZN, n = 10). * P < .05 vs vehicle-treated group; # P < .05 vs $ZnCl_2$ -treated group; & P < .05 vs NAC-treated group (one-way analysis of variance [ANOVA] followed by Bonferroni post hoc test; F: $F = 4.332, P = .01$; K: $F = 5.022, P = .005$; P: $F = 6.591, P = .001$). Q, Vesicular zinc expression in the mossy fibers (MFs) of hippocampal DG from mice treated with vehicle, $ZnCl_2$, NAC, or ZN as shown by TSQ fluorescence. Scale bar = 100 μm . R, Quantification of TSQ fluorescent intensity from the MFs of DG. Data are mean \pm SEM; n = 3 from each group, * P < .05 vs vehicle-treated group; # P < .05 vs $ZnCl_2$ -treated group; & P < .05 vs NAC-treated group (Kruskal-Wallis test followed by Bonferroni post hoc test: Chi square = 9.842, df = 3, $P = .02$). S, Representative images of the DG showing BrdU- (green) and DAPI- (blue) immunopositive cells as merged images to vehicle-, $ZnCl_2$ -, NAC-, or ZN-treated mice at 8 weeks after initial ZN supplementation. Scale bar = 20 μm . T, Quantification of BrdU⁺ cells in the SGZ/GCL (mean \pm SEM; vehicle, n = 6; $ZnCl_2$, n = 8; NAC, n = 9; ZN, n = 9). * P < .05 vs vehicle-treated group; # P < .05 vs $ZnCl_2$ -treated group; & P < .05 vs NAC-treated group (one-way ANOVA followed by Bonferroni post hoc test: $F = 12.651, P < .001$). U, Representative images of BrdU- (green) and NeuN- (red) immunopositive cells as merged images to vehicle-, $ZnCl_2$ -, NAC-, or ZN-treated mice. Scale bar = 10 μm . V, W, Bar graphs showing the number (V) and percentage (W) of cells that express the markers BrdU and NeuN (newborn neurons) in the SGZ/GCL (mean \pm SEM; vehicle, n = 6; $ZnCl_2$, n = 8; NAC, n = 9; ZN, n = 9). * P < .05 vs vehicle-treated group; # P < .05 vs $ZnCl_2$ -treated group; & P < .05 vs NAC-treated group (one-way ANOVA followed by Bonferroni post hoc test; V: $F = 9.802, P < .001$; W: $F = 3.803, P = .021$)

$ZnT3^{-/-}$ mice treated with ZN or vehicle showed a lower percentage of BrdU⁺NeuN⁺ cells among BrdU⁺ cells than $ZnT3^{+/+}$ mice treated with ZN or vehicle, respectively (Figure 3L). In contrast with results obtained after administration of ZN, no significant difference in the

ratio of the number of surviving BrdU⁺ cells in the SGZ/GCL at 47 days to the number of BrdU⁺ cells in the DG at 5 days after initial BrdU injection in either $ZnT3^{+/+}$ and $ZnT3^{-/-}$ mice treated with ZN vs vehicle-treated mice, indicating that ZN does not regulate the

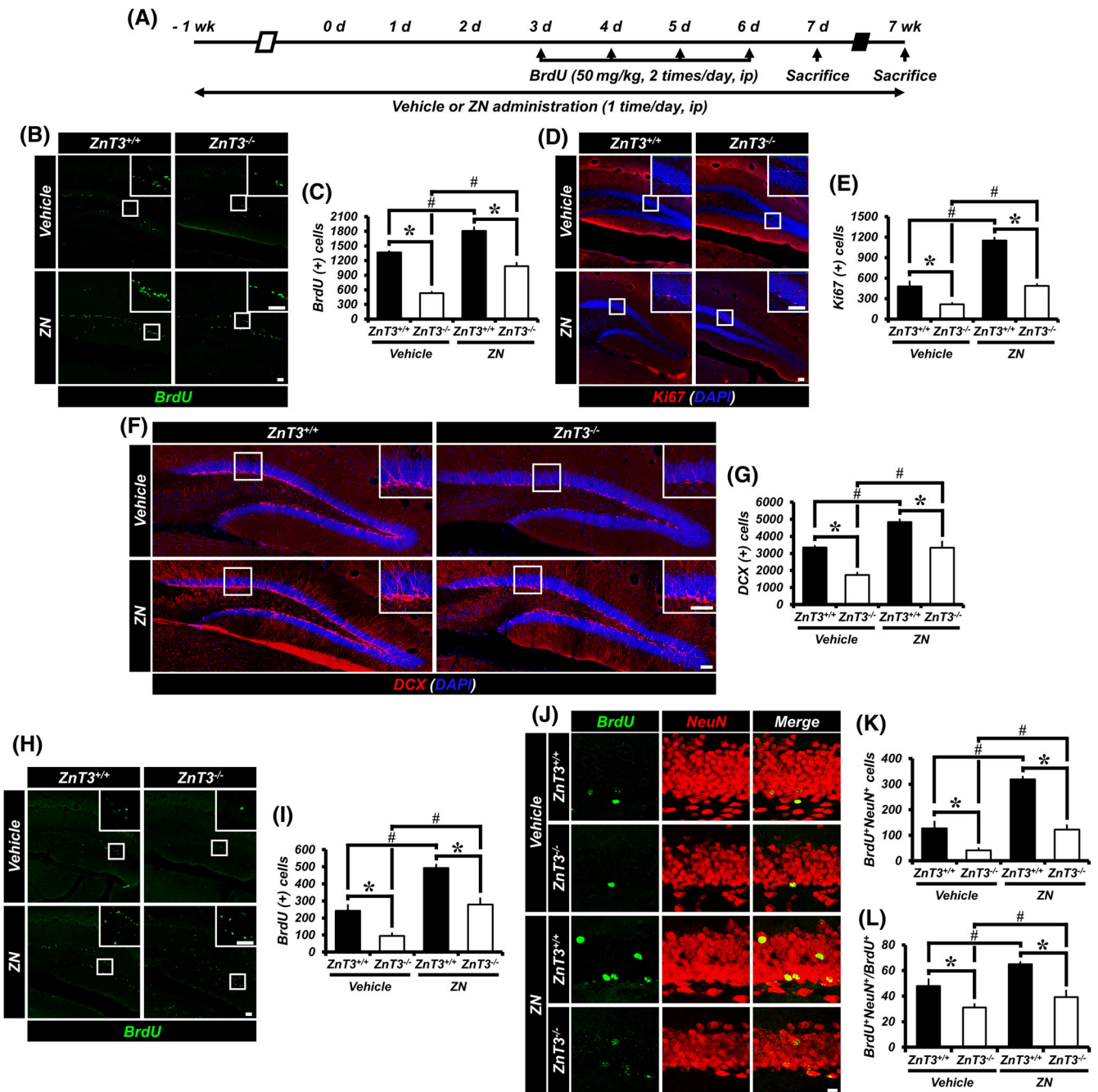


FIGURE 3 Administration of ZN in *ZnT3^{-/-}* mice increases adult hippocampal neurogenesis. A, Timeline showing the experimental design. B, Representative images of the DG showing BrdU (green) staining from vehicle- or ZN-treated mice (either *ZnT3^{+/+}* or *ZnT3^{-/-}*) at 2 weeks after initial ZN supplementation. Scale bar = 50 μ m. C, Quantification of BrdU⁺ cells in the SGZ/GCL (mean \pm SEM; n = 6-9 from each group). **P* < .05 vs *ZnT3^{+/+}* mice; #*P* < .05 vs vehicle-treated mice (one-way ANOVA followed by Bonferroni post hoc test: *F* = 76.753, *P* < .001). D, Representative images of Ki67- (red) and DAPI- (blue) immunopositive cells as merged images from vehicle- or ZN-treated mice (either *ZnT3^{+/+}* or *ZnT3^{-/-}*). Scale bar = 50 μ m. E, Number of progenitor cells (Ki67⁺DAPI⁺) in the SGZ/GCL (mean \pm SEM; n = 6-9 from each group). **P* < .05 vs *ZnT3^{+/+}* mice; #*P* < .05 vs vehicle-treated mice (one-way ANOVA followed by Bonferroni post hoc test: *F* = 92.234, *P* < .001). F, Representative images of DCX- (red) and DAPI- (blue) immunopositive cells as merged images from vehicle- or ZN-treated mice (either *ZnT3^{+/+}* or *ZnT3^{-/-}*). Scale bar = 50 μ m. G, Number of immature neurons (DCX⁺DAPI⁺) in the SGZ/GCL (mean \pm SEM; n = 6-9 from each group). **P* < .05 vs *ZnT3^{+/+}* mice; #*P* < .05 vs vehicle-treated mice (one-way ANOVA followed by Bonferroni post hoc test: *F* = 34.601, *P* < .001). H, Representative images of the DG showing BrdU (green) staining to vehicle- or ZN-treated mice (either *ZnT3^{+/+}* or *ZnT3^{-/-}*) at 8 weeks after initial ZN supplementation. Scale bar = 50 μ m. I, Quantification of BrdU⁺ cells in the SGZ/GCL (mean \pm SEM; n = 6-8). **P* < .05 vs *ZnT3^{+/+}* mice; #*P* < .05 vs vehicle-treated mice (one-way ANOVA followed by Bonferroni post hoc test: *F* = 44.071, *P* < .001). J, Representative images of BrdU- (green) and NeuN- (red) immunopositive cells as merged images to vehicle- or ZN-treated mice (either *ZnT3^{+/+}* or *ZnT3^{-/-}*). Scale bar = 50 μ m. K,L, Bar graphs showing the number (K) and percentage (L) of cells that express the markers BrdU and NeuN (newborn neurons) in the SGZ/GCL (mean \pm SEM; n = 6-8). **P* < .05 vs *ZnT3^{+/+}* mice; #*P* < .05 vs vehicle-treated mice (one-way ANOVA followed by Bonferroni post hoc test; K: *F* = 60.390, *P* < .001; L: *F* = 24.074, *P* < .001)

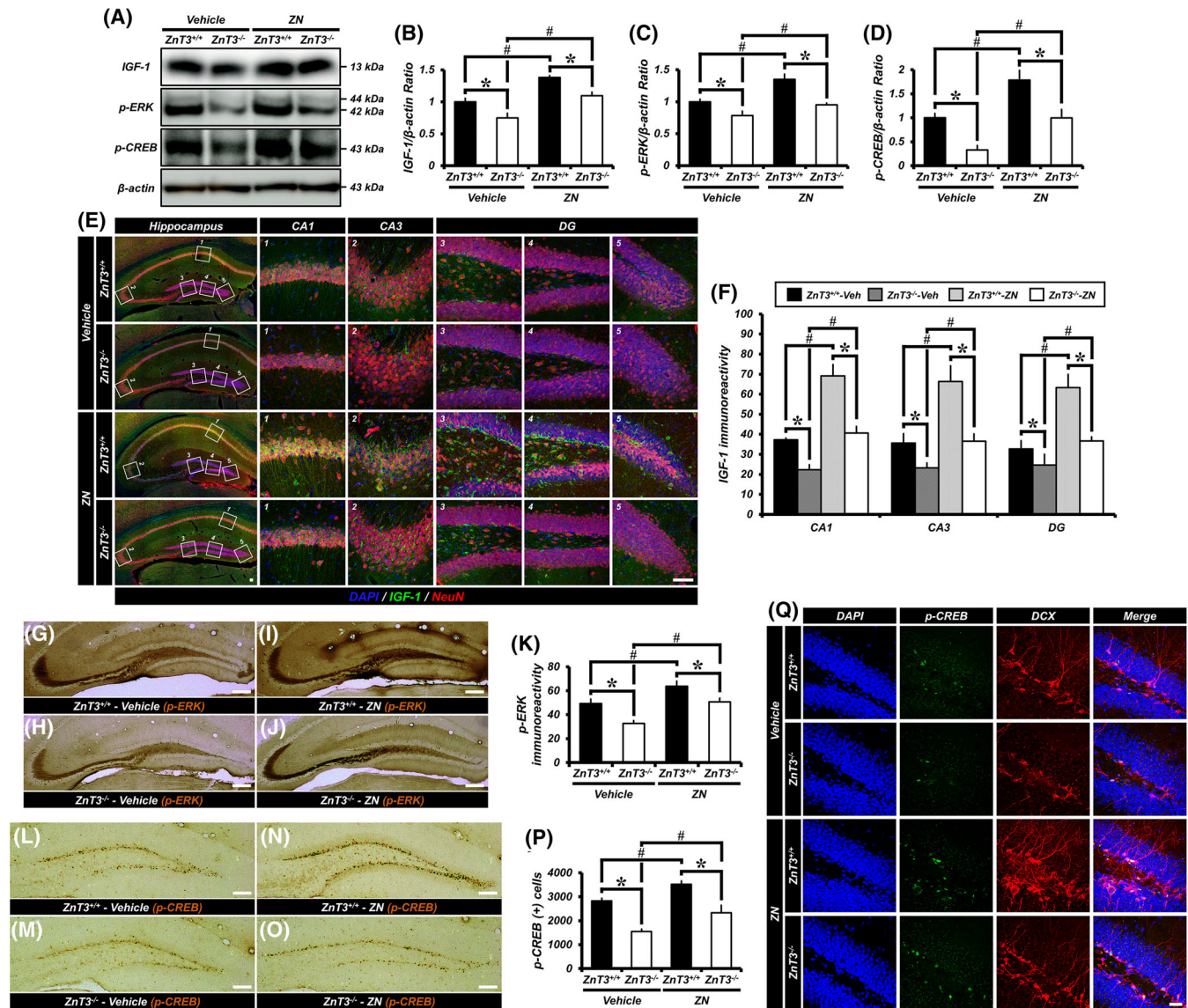


FIGURE 4 ZN increases IGF-1 expression and leads to ERK/CREB activation in the hippocampus. A, Western blotting analysis of IGF-1, pERK or pCREB in the hippocampus from either *ZnT3^{+/+}* or *ZnT3^{-/-}* mice treated with vehicle or ZN. B-D, Quantification of IGF-1 (B), pERK (C), or pCREB (D) expression from the hippocampus (mean ± SEM; n = 5 from each group). **P* < .05 vs *ZnT3^{+/+}* mice; #*P* < .05 vs vehicle-treated mice (Kruskal-Wallis test followed by Bonferroni post hoc test; B: Chi square = 9.134, df = 3, *P* = .028; C: Chi square = 14.634, df = 3, *P* = .002; D: Chi square = 14.429, df = 3, *P* = .002). E, DAPI- (blue), IGF-1- (green), and NeuN- (red) immunofluorescence in vehicle- and ZN-treated mice of either *ZnT3^{+/+}* or *ZnT3^{-/-}* genotype. Scale bar = 50 μm. F, Quantification of IGF-1 immunoreactivity in the hippocampal CA1, CA3 and DG (mean ± SEM; n = 5 from each group). **P* < .05 vs *ZnT3^{+/+}* mice; #*P* < .05 vs vehicle-treated mice (Kruskal-Wallis test followed by Bonferroni post hoc test; CA1: Chi square = 12.728, df = 3, *P* = .005; CA3: Chi square = 11.184, df = 3, *P* = .011; DG: Chi square = 12.482, df = 3, *P* = .006). G-J, Representative images showing pERK-immunopositive mossy fiber (MF) pathway to vehicle-treated *ZnT3^{+/+}* (G) and *ZnT3^{-/-}* (H) mice or ZN-treated *ZnT3^{+/+}* (I) and *ZnT3^{-/-}* (J) mice daily for 2 weeks. Scale bar = 50 μm. K, Quantification of pERK immunoreactivity in the hippocampal MF (mean ± SEM; vehicle-treated *ZnT3^{+/+}* mice, n = 7; ZN-treated *ZnT3^{+/+}* mice, n = 8; vehicle-treated *ZnT3^{-/-}* mice, n = 9; ZN-treated *ZnT3^{-/-}* mice, n = 7). **P* < .05 vs *ZnT3^{+/+}* mice; #*P* < .05 vs vehicle-treated mice. L-O, Representative images of the DG showing pCREB-immunopositive cells to vehicle-treated *ZnT3^{+/+}* (L) and *ZnT3^{-/-}* (M) mice or ZN-treated *ZnT3^{+/+}* (N) and *ZnT3^{-/-}* (O) mice daily for 2 weeks. Scale bar = 50 μm. P, Bar graph showing the number of pCREB immunopositive cells in the SGZ/GCL (mean ± SEM; vehicle-treated *ZnT3^{+/+}* mice, n = 7; ZN-treated *ZnT3^{+/+}* mice, n = 8; vehicle-treated *ZnT3^{-/-}* mice, n = 9; ZN-treated *ZnT3^{-/-}* mice, n = 7). **P* < .05 vs *ZnT3^{+/+}* mice; #*P* < .05 vs vehicle-treated mice (one-way ANOVA followed by Bonferroni post hoc test: *F* = 22.439, *P* < .001). Q, DAPI- (blue), pCREB- (green), and DCX- (red) immunofluorescence in vehicle- and ZN-treated mice of either the *ZnT3^{+/+}* or *ZnT3^{-/-}* genotype. Scale bar = 50 μm. P, phosphorylated

survival ratio of newly generated cells. However, we noted that ZN significantly increased the number of BrdU⁺ and BrdU⁺NeuN⁺ cells in the SGZ/GCL of both *ZnT3^{+/+}* and *ZnT3^{-/-}* mice compared with

vehicle-treated mice. Thus, these results demonstrate that ZN reverses the reduction in adult hippocampal neurogenesis, caused by deletion of the *ZnT3* gene.

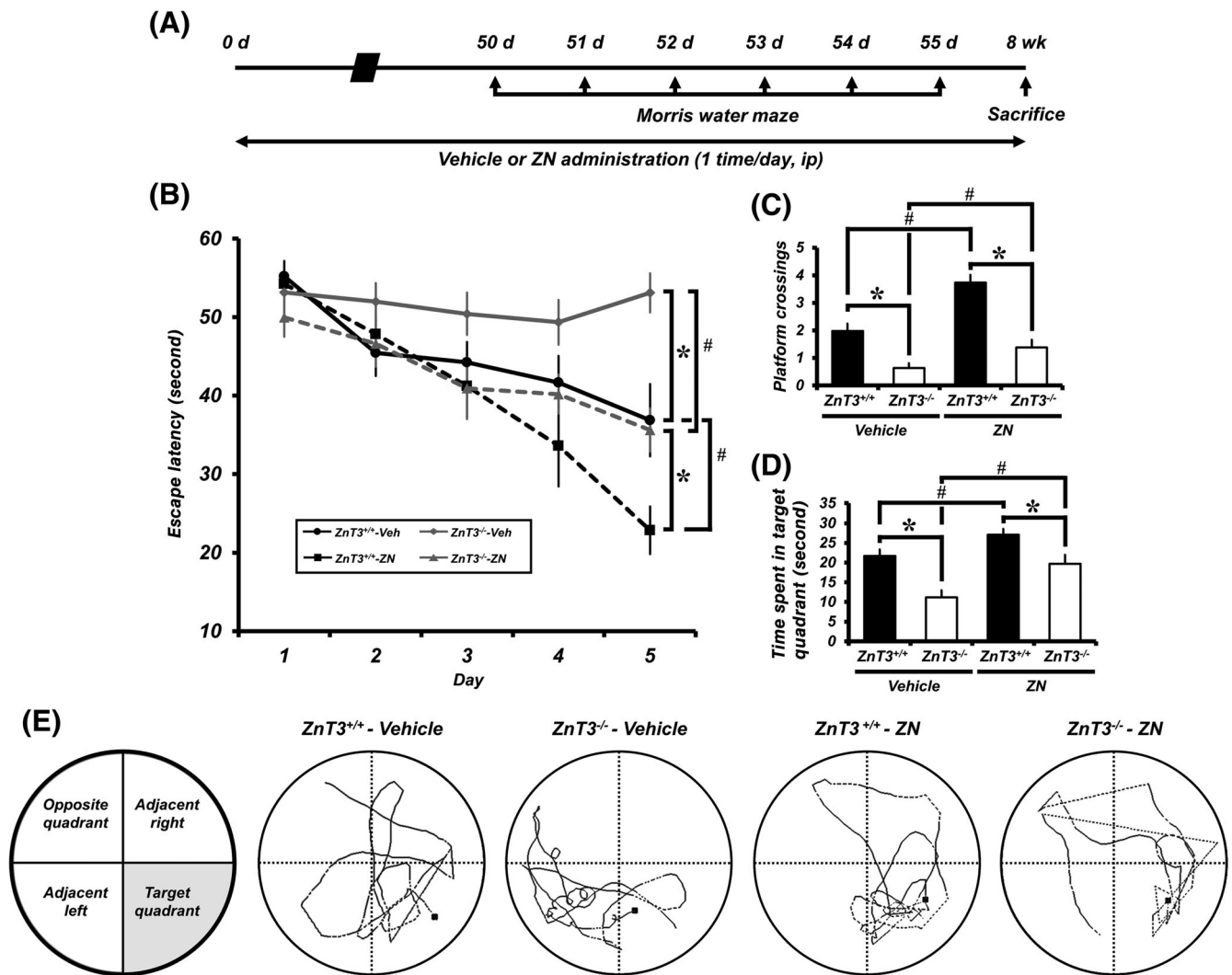


FIGURE 5 ZN improves cognitive function in aged $ZnT3^{+/+}$ and $ZnT3^{-/-}$ mice. A, Timeline showing the experimental design. B, Morris water maze (MWM) performance. Escape latency of acquisition trial for five consecutive days starting 50 days after the initial ZN supplementation (mean \pm SEM; vehicle-treated $ZnT3^{+/+}$ mice, $n = 11$; ZN-treated $ZnT3^{+/+}$ mice, $n = 12$; vehicle-treated $ZnT3^{-/-}$ mice, $n = 13$; ZN-treated $ZnT3^{-/-}$ mice, $n = 14$). * $P < .05$ vs $ZnT3^{+/+}$ mice; # $P < .05$ vs vehicle-treated mice (repeated measure ANOVA; Day: $F = 74.695$, $P < .001$; Group: $F = 7.543$, $P < .001$; Day \times Group interaction: $F = 11.120$, $P < .001$). C, MWM platform crossing. D, Time spent in target quadrant. E, Schematic diagram of tank and probe trial testing. Representative searching/swimming tracks by mice with each group in the probe trial (mean \pm SEM; vehicle-treated $ZnT3^{+/+}$ mice, $n = 11$; ZN-treated $ZnT3^{+/+}$ mice, $n = 12$; vehicle-treated $ZnT3^{-/-}$ mice, $n = 13$; ZN-treated $ZnT3^{-/-}$ mice, $n = 14$). * $P < .05$ vs $ZnT3^{+/+}$ mice; # $P < .05$ vs vehicle-treated mice (one-way ANOVA followed by Bonferroni post hoc test; C: $F = 26.412$, $P < .001$; D: $F = 13.204$, $P < .001$).

3.8 | ZN Treatment increases IGF-1 expression and ERK/CREB activation in the hippocampus

The effects of $ZnT3$ gene deletion and ZN supplementation on the expression of IGF-1 and the activity of ERK/CREB pathways were investigated to elucidate the mechanisms underlying the effect of vesicular zinc on adult hippocampal neurogenesis. It is known that IGF-1 acts to promote adult neurogenesis and that the ERK/CREB signaling pathway also plays an important role in maintaining normal levels of neurogenesis. We therefore examined IGF-1 expression in addition to measuring ERK and CREB phosphorylation (pERK and pCREB), which

are the activated forms of these molecules. Western blot revealed a significant decrease in the level of IGF-1, pERK, and pCREB proteins in the hippocampus of $ZnT3^{-/-}$ mice as compared with the $ZnT3^{+/+}$ mice. However, administration of ZN remarkably increased the protein level of IGF-1, pERK and pCREB in both $ZnT3^{+/+}$ and $ZnT3^{-/-}$ mice as compared with the vehicle-treated mice, although $ZnT3^{-/-}$ mice treated with ZN showed lower IGF-1, pERK and pCREB protein levels than $ZnT3^{+/+}$ mice (Figure 4A-D). We also observed a significant reduction of IGF-1- and pERK-IR and the number of pCREB-positive cells in $ZnT3^{-/-}$ mice compared with $ZnT3^{+/+}$ mice. However, administration of ZN remarkably increased IGF-1- and pERK-IR and pCREB⁺ cells in both

ZnT3^{+/+} and *ZnT3*^{-/-} mice, although *ZnT3*^{-/-} mice treated with ZN showed a lower IGF-1- and pERK-IR or pCREB⁺ cells than *ZnT3*^{+/+} mice treated with ZN (Figure 4E-P).

Several studies have demonstrated that the pCREB has been found to be present in the majority of newborn immature neurons in the adult DG and thus CREB signaling is known to play an important role in neuronal activation and in the survival stages of neurogenesis.¹⁷ To confirm the relationship between immature neurons and pCREB-expressing cells in the SGZ, we performed immunofluorescence staining against pCREB and DCX. Most of the pCREB⁺ cells were colocalized with DCX⁺ neuroblasts in their nuclei. We observed a significant decrease of pCREB⁺DCX⁺ cells in *ZnT3*^{-/-} mice compared with *ZnT3*^{+/+} mice. However, administration of ZN remarkably increased the number of pCREB⁺DCX⁺ cells in both *ZnT3*^{+/+} and *ZnT3*^{-/-} mice (Figure 4Q). Together, these findings provide further evidence that ERK and CREB activation were both necessary for the effect of vesicular zinc on adult hippocampal neurogenesis.

3.9 | ZN treatment improves cognitive function in aged *ZnT3*^{+/+} and *ZnT3*^{-/-} mice

To investigate whether ZN supplementation improves cognitive abilities in both aged *ZnT3*^{+/+} and *ZnT3*^{-/-} mice, mice were subjected to the MWM test for six consecutive days starting 50 days after the initial ZN supplementation. At 24 hours after the last training session, their behavior was recorded for 60 seconds after removing the platform as a probe trial (Figure 5A). The escape latency decreased progressively during 5 training days. *ZnT3*^{-/-} mice spent longer periods of time finding the platform, had a decreased number of platform crossings, and had reduced time spent in the target quadrant compared to *ZnT3*^{+/+} mice. However, ZN supplementation resulted in an improved cognitive ability in both *ZnT3*^{+/+} and *ZnT3*^{-/-} mice, as proven by a significant reduction in escape latency (Figure 5B) and an increase in the number of platform crossings (Figure 5C) and time spent in the target quadrant (Figure 5D,E) compared to the vehicle-treated mice. These results demonstrate that ZN reverses aging-dependent cognitive decline in *ZnT3*^{-/-} mice.

4 | DISCUSSION

The present study tested our hypothesis that vesicular zinc plays a central role in regulating adult neurogenesis occurring in the hippocampus. To test our hypothesis, we used mice in which vesicular zinc had been depleted by *ZnT3* gene deletion. Here we found that *ZnT3* gene deletion completely depleted vesicular zinc in the hippocampal MF tract and the number of progenitor cells, neuroblasts, and newborn neurons were remarkably reduced in the *ZnT3*^{-/-} mice, even under physiological conditions. In addition, we also found that zinc supplementation with ZN reversed the reduction of adult neurogenesis in *ZnT3*^{-/-} mice. This defective adult neurogenesis is due to a cell-extrinsic mechanism of *ZnT3* deficiency and is accompanied by

reduced levels of pERK and pCREB in the hippocampus of *ZnT3*^{-/-} mice. The present study also demonstrated that IGF-1 expression is lower in the hippocampus of *ZnT3*^{-/-} mice than wild type mice. Reduction of the level of IGF-1 is reversed by ZN supplementation in both *ZnT3*^{+/+} and *ZnT3*^{-/-} mice, which suggests that *ZnT3* is involved in IGF-dependent neurogenesis in the brain. Thus, these findings describe a central function for *ZnT3* in maintaining adult hippocampal neurogenesis.

A possible relationship between zinc and hippocampal neurogenesis after brain injury has been reported by our previous studies. Our previous study suggests that decreased vesicular zinc content in the MF terminals of dentate granule neurons may cause impaired progenitor cell proliferation.¹⁵ We also reported that zinc chelation by clioquinol (5-chloro-7-iodo-8-hydroxyquinoline; CQ) reduced hippocampal progenitor cell proliferation and neurogenesis after hypoglycemia, traumatic brain injury, and seizure.^{15,18,19} Supporting these findings, we recently demonstrated that enhancing hippocampal vesicular zinc via zinc supplementation with ZC increased hippocampal vesicular zinc concentration and thereby promotes adult neurogenesis under physiological²⁰ or pathological conditions such as diabetes.²¹ These results support the notion that zinc is a critical regulator of adult neurogenesis.

Our previous studies demonstrated that zinc-deficient diet reduced zinc concentration in the presynaptic hippocampal vesicles in rats fed a zinc-deficient diet and that these mice showed reduced hippocampal neurogenesis.¹⁵ A separate group also reported that dietary zinc deprivation caused impaired cognitive function.^{8,22} However, the precise mechanism that leads to cognitive impairment in zinc-deficient animals is still unknown. Several laboratories have shown that *ZnT3* gene deletion mice exhibit age-dependent deficits in learning and memory,⁹ impaired contextual discrimination, and spatial working memory¹⁰ and are deficient in social and object recognition memory.¹¹ McAllister et al. demonstrated that *ZnT3*^{-/-} mice did not appear to readily develop the usual depression-like effects that occur after stress but however, were not completely free of stress-induced dysfunction,²³ as fear memory generation was enhanced by stress in *ZnT3*^{-/-} mice. Although the stress response is affected by *ZnT3* gene deletion, hippocampal cellular proliferation was not significantly disrupted by stress in CD1 background mice. This group recently demonstrated that *ZnT3*^{-/-} mice showed increased basal dendritic length in the cerebral cortex, which is not affected by housing condition.²⁴ Thus, these studies suggest that *ZnT3* and vesicular zinc are involved in certain types of spatial memory and behavior that are dependent on the background strain or on different stress conditions during development. We believe that further study will be needed to evaluate this difference as suggested.^{25,26}

From the above studies, including our works, we hypothesized that a zinc deficient-induced cognitive impairment may be associated with a decline in hippocampal neurogenesis. Zinc-deficient diet not only affects hippocampal vesicular zinc concentration but also affects systemic zinc levels, including blood and cerebrospinal fluid (CSF) in the brain. For this reason, we cannot differentiate whether the dietary zinc-deficient-induced cognitive impairment is solely affected by

decreased hippocampal neurogenesis. Thus, to test our hypothesis we used *ZnT3*^{-/-} mice, which contain no vesicular zinc in the presynaptic terminal of hippocampus and cerebral cortex due to an inability to package zinc into synaptic vesicles.^{27,28} The basal level of BrdU-, Ki67-, and DCX-immunopositive cells was significantly diminished in *ZnT3*^{-/-} mice compared with *ZnT3*^{+/+} mice. These results suggest that vesicular zinc originating from synaptic vesicles is necessary for progenitor cell proliferation and neuronal differentiation.

Why *ZnT3*^{-/-} mice develop cognitive impairment during aging is not clear. Sindreu et al showed that *ZnT3*^{-/-} mice have reduced activation of the ERK1/2 mitogen-activated protein kinase (MAPK) in hippocampal MF terminals and reduced inhibition of the zinc-sensitive tyrosine phosphatase MAPK in the setting of hippocampus-dependent learning.¹⁰ They suggested that a deficit of ERK signaling in *ZnT3*^{-/-} mice caused impaired contextual discrimination, which is a possible mechanism of memory impairment of these mice. ERK signaling is also important for hippocampal neurogenesis and presynaptic pERK also modulates MF plasticity.²⁹ Zinc can promote transcription of the BDNF gene and zinc supplementation increases the expression of BDNF mRNA in the adult rat brain.³⁰ The zinc finger transcription factor CREB can stimulate transcription of BDNF.³¹ Currently, it is unknown how zinc induced BDNF expression occurs. One line of potential evidence to explain this phenomenon is the observation that zinc deficiency leads to a decreased phosphorylation of CREB in mice,³² which indicates that zinc could modulate CREB activity. ERK1/2 phosphorylates the kinases RSK and MSK, which can directly phosphorylate CREB.³³ Zinc might stimulate CREB to increase the expression of BDNF via activation of ERK1/2, potentially forming a positive feedback loop to further activate local ERK1/2 signaling as an autocrine or paracrine factor. These results may explain why *ZnT3*^{-/-} mice showed depressed progenitor cell proliferation and neurogenesis.

Studies using *ZnT3*^{-/-} mice have produced mixed results with respect to how BDNF levels in the brain are affected by this manipulation. Several labs have reported that no difference exists between *ZnT3*^{+/+} and *ZnT3*^{-/-} mice.^{9,24} On the other hand, other researchers have demonstrated that *ZnT3*^{-/-} mice showed increased levels of hippocampal BDNF.^{34,35} Therefore, as an alternative line of investigation into whether neurotrophic factors are impacted by manipulation of zinc transporter function, the present study sought to explore IGF-1 levels in both *ZnT3*^{+/+} and *ZnT3*^{-/-} mice treated with or without ZN supplementation. We found that IGF-1 levels in the hippocampus were reduced in *ZnT3*^{-/-} mice, compared to *ZnT3*^{+/+} mice, which was reversed by ZN supplementation. Increased expression of IGF-1 and ERK phosphorylation during hippocampal neurogenesis has been suggested as potential mechanisms for these effects.³⁶⁻⁴⁰ However, subsequent studies are needed to elucidate how the observed decrease in ERK and CREB phosphorylation via IGF-1 arises from *ZnT3* gene deletion.

One factor that can influence cellular differentiation is the redox potential. It is known to dynamically change as cells differentiate; for instance, it has been shown that the level of superoxide radicals increases as cells move from G1 to M phase.⁴¹ Additionally, concentrations of hydrogen peroxide and superoxide play a role in the choice to either enter or exit the cell cycle.⁴² In support of these

observations, we previously demonstrated that newly generated neurons are exposed to oxidative stress at specific developmental timepoints, potentially explaining effects on hippocampal neurogenesis⁴³ observed in these animals. To test this, we used ZN which is zinc chloride mixed with NAC in 1:2 M ratio to increase brain zinc and cysteine levels. NAC, a glutathione precursor, is known to be a membrane-permeant cysteine prodrug with potent antioxidant, anti-inflammatory properties, and proneurogenesis. Strikingly, we observed increased pERK and pCREB expression in the hippocampus of both *ZnT3*^{+/+} and *ZnT3*^{-/-} mice treated with ZN, thereby increasing adult hippocampal neurogenesis. This indicates that ZN supplementation has uniquely beneficial effects in that it can enhance de novo synthesis and also protect against the loss of newborn neurons.

The present study has potential limitations that need to be addressed in future studies. Here we found that zinc supplementation by ZN significantly increased not only hippocampal vesicular zinc levels but also neurogenesis. According to our results, the present study suggests that vesicular zinc is critical for adult hippocampal neurogenesis. However, ZN treatment did not affect vesicular zinc levels in the *ZnT3*^{-/-} mice, which completely depleted vesicular zinc in the hippocampal MFs, suggesting the possibility that not only vesicular zinc but also extracellular zinc can promote neurogenesis. So, we cannot exclude the possibility that brain can use extracellular zinc arising from blood and CSF to maintain neurogenesis. Thus, exploring the effect of zinc supplementation by ZN on extracellular zinc concentrations could be a future direction for research that not only vesicular zinc but also extracellular zinc can promote adult hippocampal neurogenesis. The results presented here of defective adult neurogenesis in the DG of *ZnT3*^{-/-} mice and decreased pERK and pCREB expression thus raise the intriguing possibility that this adult hippocampal *ZnT3*-related phenotype reflects aging-dependent cognitive decline in *ZnT3*^{-/-} mice. However, future investigation will be surely be required to dissect the molecular and cellular events that underlie decreased ERK and CREB phosphorylation seen after genetic deletion of *ZnT3*.

5 | CONCLUSION

Together, the results from this study indicate that *ZnT3* has a central function in maintaining adult hippocampal neurogenesis and zinc supplementation by ZN has a beneficial effect on hippocampal neurogenesis and may serve as a therapeutic target for enhanced neuroprotection and repair after injury. Therefore, the present study suggests that vesicular zinc is a critical regulator of adult hippocampal neurogenesis, under physiologic conditions.

ACKNOWLEDGMENTS

This study was supported by funding from the National Research Foundation of Korea (NRF) (NRF-2019R1A2C4004912) to B.Y.C. Additionally, this work was supported by the Brain Research Program through the NRF, funded by the Ministry of Science, Information and Communication Technology and Future Planning (NRF-2017M3C7A1028937 and 2020R1A2C2008480) to S.W.S.

CONFLICT OF INTEREST

The authors declared no potential conflicts of interest.

AUTHOR CONTRIBUTIONS

B.Y.C.: conception and design, financial support, collection, and assembly of data, data analysis and interpretation, manuscript writing; D.K.H., J.H.J., B.E.L.: collection and assembly of data; J.Y.K.: data analysis and interpretation, provision of study material or patients; S.W.S.: conception and design, financial support, data analysis and interpretation, manuscript writing, final approval of manuscript.

DATA AVAILABILITY STATEMENT

The data that support the findings of this study are available on request from the corresponding author.

ORCID

Sang Won Suh  <https://orcid.org/0000-0002-7492-579X>

REFERENCES

- Frederickson CJ, Suh SW, Silva D, Frederickson CJ, Thompson RB. Importance of zinc in the central nervous system: the zinc-containing neuron. *J Nutr.* 2000;130:1471S-1483S.
- Colvin RA, Holmes WR, Fontaine CP, Maret W. Cytosolic zinc buffering and muffling: their role in intracellular zinc homeostasis. *Metallomics.* 2010;2:306-317.
- Jo SM, Danscher G, Daa Schroder H, et al. Zinc-enriched (ZEN) terminals in mouse spinal cord: immunohistochemistry and autoradiography. *Brain Res.* 2000;870:163-169.
- Ming GL, Song H. Adult neurogenesis in the mammalian central nervous system. *Annu Rev Neurosci.* 2005;28:223-250.
- MacDonald RS. The role of zinc in growth and cell proliferation. *J Nutr.* 2000;130:1500S-1508S.
- Swenerton H, Shrader R, Hurley LS. Zinc-deficient embryos: reduced thymidine incorporation. *Science.* 1969;166:1014-1015.
- Stewart GR, Frederickson CJ, Howell GA, Gage FH. Cholinergic denervation-induced increase of chelatable zinc in mossy-fiber region of the hippocampal formation. *Brain Res.* 1984;290:43-51.
- Golub MS, Takeuchi PT, Keen CL, Gershwin ME, Hendrickx AG, Lonnerdal B. Modulation of behavioral performance of prepubertal monkeys by moderate dietary zinc deprivation. *Am J Clin Nutr.* 1994; 60:238-243.
- Adlard PA, Parncutt JM, Finkelstein DI, Bush AI. Cognitive loss in zinc transporter-3 knock-out mice: a phenocopy for the synaptic and memory deficits of Alzheimer's disease? *J Neurosci.* 2010;30: 1631-1636.
- Sindreu C, Palmiter RD, Storm DR. Zinc transporter ZnT-3 regulates presynaptic Erk1/2 signaling and hippocampus-dependent memory. *Proc Natl Acad Sci USA.* 2011;108:3366-3370.
- Martel G, Hevi C, Kane-Goldsmith N, Shumyatsky GP. Zinc transporter ZnT3 is involved in memory dependent on the hippocampus and perirhinal cortex. *Behav Brain Res.* 2011;223:233-238.
- Kilkenny C, Browne WJ, Cuthill IC, et al. Improving bioscience research reporting: the ARRIVE guidelines for reporting animal research. *PLoS Biol.* 2012;8:e1000412.
- Choi BY, Hong DK, Suh SW. ZnT3 gene deletion reduces colchicine-induced dentate granule cell degeneration. *Int J Mol Sci.* 2017;18:2189-2201.
- Gundersen HJ, Bendtsen TF, Korbo L, et al. Some new, simple and efficient stereological methods and their use in pathological research and diagnosis. *APMIS.* 1988;96:379-394.
- Suh SW, Won SJ, Hamby AM, et al. Decreased brain zinc availability reduces hippocampal neurogenesis in mice and rats. *J Cereb Blood Flow Metab.* 2009;29:1579-1588.
- Faul F, Erdfelder E, Buchner A, Lang AG. Statistical power analyses using G*power 3.1: tests for correlation and regression analyses. *Behav Res Methods.* 2009;41:1149-1160.
- Nakagawa S, Kim JE, Lee R, et al. Localization of phosphorylated cAMP response element-binding protein in immature neurons of adult hippocampus. *J Neurosci.* 2002;22:9868-9876.
- Kim JH, Jang BG, Choi BY, et al. Zinc chelation reduces hippocampal neurogenesis after pilocarpine-induced seizure. *PLoS One.* 2012;7: e48543.
- Choi BY, Kim JH, Kim HJ, et al. Zinc chelation reduces traumatic brain injury-induced neurogenesis in the subgranular zone of the hippocampal dentate gyrus. *J Trace Elem Med Biol.* 2014;28:474-481.
- Choi BY, Kim IY, Kim JH, et al. Zinc plus cyclo-(his-pro) promotes hippocampal neurogenesis in rats. *Neuroscience.* 2016;339:634-643.
- Choi BY, Kim IY, Kim JH, et al. Administration of zinc plus cyclo-(his-pro) increases hippocampal neurogenesis in rats during the early phase of streptozotocin-induced diabetes. *Int J Mol Sci.* 2017;18:73-86.
- Takeda A, Takefuta S, Okada S, Oku N. Relationship between brain zinc and transient learning impairment of adult rats fed zinc-deficient diet. *Brain Res.* 2000;859:352-357.
- McAllister BB, Wright DK, Wortman RC, et al. Elimination of vesicular zinc alters the behavioural and neuroanatomical effects of social defeat stress in mice. *Neurobiol Stress.* 2018;9:199-213.
- McAllister BB, Thackray SE, de la Orta BKG, et al. Effects of enriched housing on the neuronal morphology of mice that lack zinc transporter 3 (ZnT3) and vesicular zinc. *Behav Brain Res.* 2020;379: 112336.
- McAllister BB, Dyck RH. A new role for zinc in the brain. *Elife.* 2017; 6:e31816.
- McAllister BB, Pochakom A, Fu S, et al. Effects of social defeat stress and fluoxetine treatment on neurogenesis and behavior in mice that lack zinc transporter 3 (ZnT3) and vesicular zinc. *Hippocampus.* 2019.
- Cole TB, Wenzel HJ, Kafer KE, Schwartzkroin PA, Palmiter RD. Elimination of zinc from synaptic vesicles in the intact mouse brain by disruption of the ZnT3 gene. *Proc Natl Acad Sci USA.* 1999;96: 1716-1721.
- Palmiter RD, Cole TB, Quaife CJ, Findley SD. ZnT-3, a putative transporter of zinc into synaptic vesicles. *Proc Natl Acad Sci USA.* 1996;93: 14934-14939.
- Vara H, Onofri F, Benfenati F, Sassoe-Pognetto M, Giustetto M. ERK activation in axonal varicosities modulates presynaptic plasticity in the CA3 region of the hippocampus through synapsin I. *Proc Natl Acad Sci USA.* 2009;106:9872-9877.
- Cieslik K, Sowa-Kucma M, Ossowska G, et al. Chronic unpredictable stress-induced reduction in the hippocampal brain-derived neurotrophic factor (BDNF) gene expression is antagonized by zinc treatment. *Pharmacol Rep.* 2011;63:537-543.
- Minichiello L. TrkB signalling pathways in LTP and learning. *Nat Rev Neurosci.* 2009;10:850-860.
- Gao HL, Xu H, Xin N, Zheng W, Chi ZH, Wang ZY. Disruption of the CaMKII/CREB signaling is associated with zinc deficiency-induced learning and memory impairments. *Neurotox Res.* 2011;19:584-591.
- Impey S, Obrietan K, Wong ST, et al. Cross talk between ERK and PKA is required for Ca²⁺ stimulation of CREB-dependent transcription and ERK nuclear translocation. *Neuron.* 1998;21:869-883.
- Helgager J, Huang YZ, McNamara JO. Brain-derived neurotrophic factor but not vesicular zinc promotes TrkB activation within mossy fibers of mouse hippocampus in vivo. *J Comp Neurol.* 2014;522: 3885-3899.
- Yoo MH, Kim TY, Yoon YH, Koh JY. Autism phenotypes in ZnT3 null mice: involvement of zinc dyshomeostasis, MMP-9 activation and BDNF upregulation. *Sci Rep.* 2016;6:28548.

36. O'Kusky JR, Ye P, D'Ercole AJ. Insulin-like growth factor-I promotes neurogenesis and synaptogenesis in the hippocampal dentate gyrus during postnatal development. *J Neurosci.* 2000;20:8435-8442.
37. Anderson MF, Aberg MA, Nilsson M, et al. Insulin-like growth factor-I and neurogenesis in the adult mammalian brain. *Brain Res Dev Brain Res.* 2002;134:115-122.
38. Lichtenwalner RJ, Forbes ME, Sonntag WE, Riddle DR. Adult-onset deficiency in growth hormone and insulin-like growth factor-I decreases survival of dentate granule neurons: insights into the regulation of adult hippocampal neurogenesis. *J Neurosci Res.* 2006;83:199-210.
39. Nieto-Estevez V, Oueslati-Morales CO, Li L, et al. Brain insulin-like growth factor-I directs the transition from stem cells to mature neurons during postnatal/adult hippocampal neurogenesis. *STEM CELLS.* 2016;34:2194-2209.
40. Morel GR, Leon ML, Uriarte M, et al. Therapeutic potential of IGF-I on hippocampal neurogenesis and function during aging. *Neurogenesis (Austin).* 2017;4:e1259709.
41. Menon SG, Goswami PC. A redox cycle within the cell cycle: ring in the old with the new. *Oncogene.* 2007;26:1101-1109.
42. Menon SG, Sarsour EH, Spitz DR, et al. Redox regulation of the G1 to S phase transition in the mouse embryo fibroblast cell cycle. *Cancer Res.* 2003;63:2109-2117.
43. Choi BY, Won SJ, Kim JH, et al. EAAC1 gene deletion reduces adult hippocampal neurogenesis after transient cerebral ischemia. *Sci Rep.* 2018;8:6903.

SUPPORTING INFORMATION

Additional supporting information may be found online in the Supporting Information section at the end of this article.

How to cite this article: Choi BY, Hong DK, Jeong JH, Lee BE, Koh J-Y, Suh SW. Zinc transporter 3 modulates cell proliferation and neuronal differentiation in the adult hippocampus. *Stem Cells.* 2020;38:994-1006. <https://doi.org/10.1002/stem.3194>